Science Bulletin xxx (xxxx) xxx

Contents lists available at ScienceDirect

Science Bulletin

journal homepage: www.elsevier.com/locate/scib

Review

Decadal climate variability during the pre-industrial Common Era: characteristics and mechanisms

Liang Ning [a,b,c,d,e], Zhengyu Liu [f,*], Michael E. Mann [g,*], Jian Liu [a,b,c,d,e,h,*], Mi Yan [a,b,c,d,e], Weiyi Sun [a,b,c,d,e], Kefan Chen [a,b,c,d,e], Yanmin Qin [a,b,c,d,e], Qin Wen [a,b,c,d,e]

[a] State Key Laboratory of Climate System Prediction and Risk Management, Nanjing 210023, China
[b] Key Laboratory for Virtual Geographic Environment, Ministry of Education, Nanjing 210023, China
[c] State Key Laboratory Cultivation Base of Geographical Environment Evolution and Regional Response of Jiangsu Province, Nanjing 210023, China
[d] Jiangsu Center for Collaborative Innovation in Geographical Information Resource Development and Application, Nanjing 210023, China
[e] School of Geography, Nanjing Normal University, Nanjing 210023, China
[f] Department of Geography, The Ohio State University, Columbus, OH 43210, USA
[g] Department of Earth and Environmental Science, Annenberg School for Communication, University of Pennsylvania, Philadelphia, PA 19104, USA
[h] Jiangsu Provincial Key Laboratory for Numerical Simulation of Large Scale Complex Systems, School of Mathematical Science, Nanjing Normal University, Nanjing 210023, China

ARTICLE INFO

Article history:
Received 1 December 2024
Received in revised form 5 March 2025
Accepted 6 March 2025
Available online xxxx

Keywords:
Decadal climate variability
Pre-industrial Common Era
Internal variability
External forcings

ABSTRACT

In this article, we present a comprehensive review of decadal to multi-decadal climate variability during the Common Era (CE), focusing on their characteristics and mechanisms. We begin by summarizing recent advances in proxy reconstructions that reveal the paleo-evidence of decadal to multi-decadal climate variability during the CE.

Decadal to multi-decadal variability has been observed in extensive sets of proxy records in the CE. Despite improvements in proxy records in the type, temporal resolution, and temporal coverage, there remains a lack of clear consistency in the preferred time scales and phases of the variability among different records. The agreements of decadal characteristics between proxy records and model simulations are higher during the periods with strong external forcings, but lower during periods of weak external forcing. We subsequently describe the recent modeling studies on the influences of external forcings and internal variability on decadal to multi-decadal climate variability with associated physical mechanisms, and some emerging research topics. Despite the improved understanding of climate variability and regional climate changes, especially over the eastern Asia summer monsoon region, several inconsistencies still exist, such as the amplitudes of responses to external forcings and relative contributions from external forcings and internal variability. The review ends with perspectives for future directions to reconcile discrepancies of decadal climate variability, such as applications of paleoclimate data assimilation and isotope-enabled transient climate modeling, and implications for projecting future decadal to multi-decadal climate changes and for improving the accuracy of decadal predictions.

1. Introduction

There is a growing interest in decadal to multi-decadal climate variability, hereafter simply referred to as decadal climate variability unless otherwise specified. Decadal climate variability has a large impact on global and regional social-economic developments [1]. Currently, decadal climate variability is the key topic of several international science programs, such as the PAGES2k Network, CLIVAR Decadal Climate Variability and Predictability (DCVP), CMIP6 Decadal Climate Prediction Project (DCPP), and World Climate Research Programme (WCRP). However, there remains considerable uncertainty regarding the nature of decadal climate variability, including the existence of decadal oscillations that are distinct from the red noise background, the relative contributions from internal variability and external forcings, and the predictability of decadal variability [2].

One limitation on our understanding is the relatively short length of instrumental observations, few of which date back fur-

* Corresponding authors.
E-mail addresses: liu.7022@osu.edu (Z. Liu), mmann00@sas.upenn.edu (M.E. Mann), jliu@njnu.edu.cn (J. Liu).

https://doi.org/10.1016/j.scib.2025.04.056

ther than the mid-19th century. The instrumental period of ~150 years includes only a few "cycles" of multi-decadal variability, making it challenging to extract unique features of decadal variability with high statistical significance. The pre-instrumental or pre-industrial Common Era (CE) provides a unique opportunity to address many of the key scientific questions relevant to decadal climate changes and climate dynamics [3]. First, the length of proxy records in the CE is about ten times longer than the instrumental observations, providing a larger sample size to analyze the statistical characteristics of decadal climate changes. Second, there are substantial external forcings during CE, notably the large volcanic eruptions, and this could be used to investigate the responses of climate systems to external forcing. However, the uncertainties and potential limitations associated with climate data and the drivers of climate change pose their own challenges. In this paper, we review the current status of our understanding of decadal changes during the CE in observations and model simulations, with a focus on their characteristics and underlying mechanisms. While extensive reviews exist on decadal variability during the modern instrumental era [4–6], there are fewer such reviews of the pre-instrumental period. Here we will focus on this longer time frame. We review evidence documenting the characteristics of decadal variability in the Pacific and Atlantic, as well as decadal changes associated with El Niño-southern oscillation (ENSO) and the monsoon systems. We discuss distinct features of the mechanisms of decadal variability in the pre-industrial CE.

2. Paleo evidence from proxy reconstructions

2.1. Global temperature and hydroclimate

Currently, there are several reconstructions of global temperature and hydroclimate covering the CE, which facilitate the analyses of historical decadal to multidecadal variability. Using a set of over a thousand proxy records consisting of tree-ring, ice core, coral, speleothem, and lake and ocean sediment data over the global ocean and land regions, Mann et al. [7] used a climate field reconstruction approach to reconstruct the surface temperature field of the past 1500 years over the globe. Then, with updated and screened temperature-sensitive paleoclimate proxy records, the PAGES 2k Consortium applied a variety of statistical methods including data assimilation to reconstruct global and hemispheric mean surface temperature over the past 2000 years [8].

Besides these reconstructions based mainly on proxy records, Tardif et al. [9] instead employed a data assimilation approach to combine model simulations with proxy records, with more realistic proxy system models taking seasonality and temperature/moisture sensitivity into account, to reconstruct past global temperature variability over this timeframe, a.k.a., the last millennium reanalysis (LMR). In addition to these reconstructions mainly focusing on temperature, Steiger et al. [10] further generated the global reconstructions of hydroclimate and associated dynamical variables covering the last millennia, a.k.a., the Paleo Hydrodynamics Data Assimilation (PHYDA).

These reconstructions exhibit similarity in long-term trends and timing of multidecadal variability, but relatively reduced agreements on amplitudes of multidecadal variability, likely owing to the different methods and data used. When data assimilation is applied, for example, and the modeled and reconstructed temperatures disagree, one tends to get an intermediate and smoothed-out result, consistent with the relative absence of multidecadal variability in the resulting global temperature reconstruction. Similarly, when an average over multiple reconstructions is performed, there is a tendency for loss of variance (Fig. 1a).

The proxy reconstructions and model simulations show agreement on the timing and magnitude of multidecadal (larger than 30 years) GMST variability between 1300 and 1800 CE, suggesting a dominant influence from external forcing on multidecadal GMST variability [11]. These agreements reduce during the periods with lower-quality external forcings used in model simulations [8] or dominated by internal variability [11]. However, how much current models could realistically reproduce the relative magnitudes of internal multidecadal GMST variability remains controversial [8]. Furthermore, larger uncertainties exist in shorter-term decadal (<30 years) GMST variability, which are more sensitive to dating uncertainties of proxy records and simulated responses to external forcings. The agreements between proxy records and model simulations on decadal to multidecadal regional temperature variability require further examination, because of the sparse distributions of proxy records and complex simulated regional responses. Meanwhile, different from temperature reconstructions, similar evaluations of hydroclimate reconstructions and potential sources of uncertainties remain limited, with only a few recent studies focusing on drought indices [9,10].

In summary, during the CE, proxy reconstructions and model simulations show high confidence in the timing of multidecadal GMST variability induced by external forcings, and medium confidence in the magnitudes either between proxy reconstructions and model simulations or among different reconstructions. While for the unforced multidecadal GMST variability, there are only qualitative agreements on the magnitude of this variability between proxy reconstructions and model simulations. Further investigations are needed in the future for shorter-term decadal GMST variability, decadal to multidecadal regional temperature variability and hydroclimate variability, and influences from uncertainties of reconstructions and model simulations.

2.2. Pacific decadal variability (PDV)

The PDV, has been defined as the leading mode of SST over subtropical North Pacific (20°–70°N) of preferred time scale of decadal to multi-decadal [12], though this can be sensitive to the assumptions behind how that is defined apparent in the historical period (Fig. 2a). Its origins likely lie in a combination of different physical processes, including North Pacific atmosphere-ocean interactions, the extratropical response to variability originating in the equatorial Pacific [12] and the response to changing natural and anthropogenic radiative forcing [2,13]. PDV has also been described in terms of several climate modes, such as the Interdecadal Pacific Oscillation (IPO), the Pacific Decadal Oscillation (PDO), the North Pacific Gyre Oscillation (NPGO), and the South Pacific Decadal Oscillation (SPDO), which are identified through principal component analysis of low-frequency climate in different domains [5]. Recent studies also found that PDV is highly correlated with tropical Pacific decadal variability (TPDV) through ENSO teleconnections and extratropical atmospheric forcing [14].

PDV during the pre-industrial CE has often been reconstructed based on tree-ring records from North America [15] and East Asia [16]. Besides tree-ring records, coral oxygen isotope and Sr/Ca over the South Pacific Convergence Zone [17], annual snowfall and sea-salt concentration records from Law Dome (East Antarctica) [18], and ice core oxygen isotope records from Tibetan Plateau [19] were also used to reconstruct the historical PDV variations (Fig. 1b). In addition to these reconstructions on separate regions, the tree-ring data from trans-Pacific region [20], and the principal components of oxygen isotopic ratio, net accumulation, and dust concentrations from four ice cores around the Pacific basin [21] were further employed to reconstruct the PDV variations considering its basin-wide impacts.

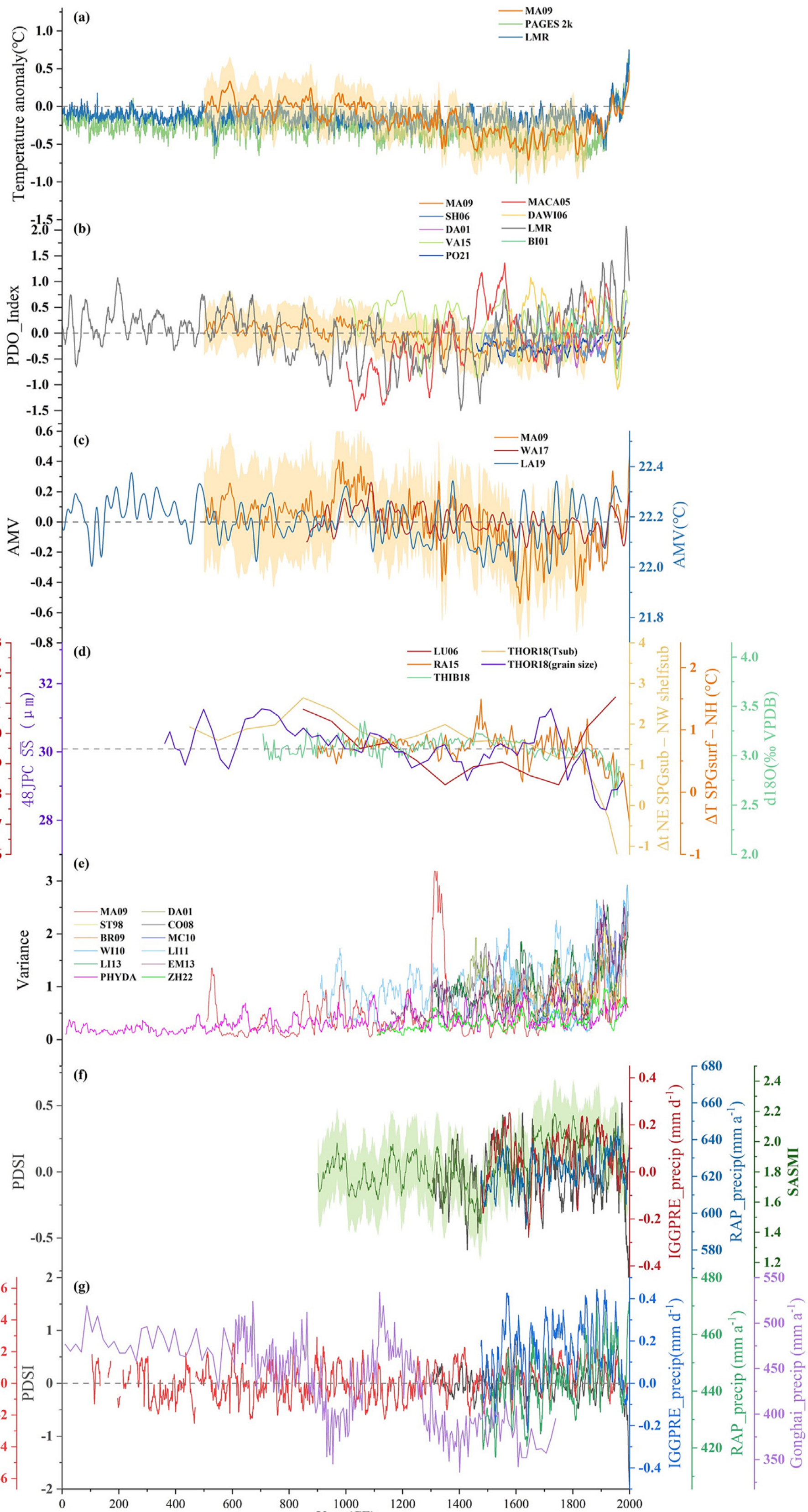

Fig. 1. Reconstructions of decadal surface temperature over the Northern Hemisphere (a), PDV (b), AMV (c), AMOC (d), ENSO decadal variance (e), SASM (f), and EASM (g) during the CE. (a) Reconstructions of decadal surface temperature over the Northern Hemisphere. (b) Reconstructions of PDV (PDO/IPO) time series. (c) Reconstructions of AMV time series. (e) Reconstructions of ENSO decadal variance. (f) Reconstructions of SASM. (g) Reconstructions of EASM. The detailed information on these reconstructions is listed in Table S1 online.

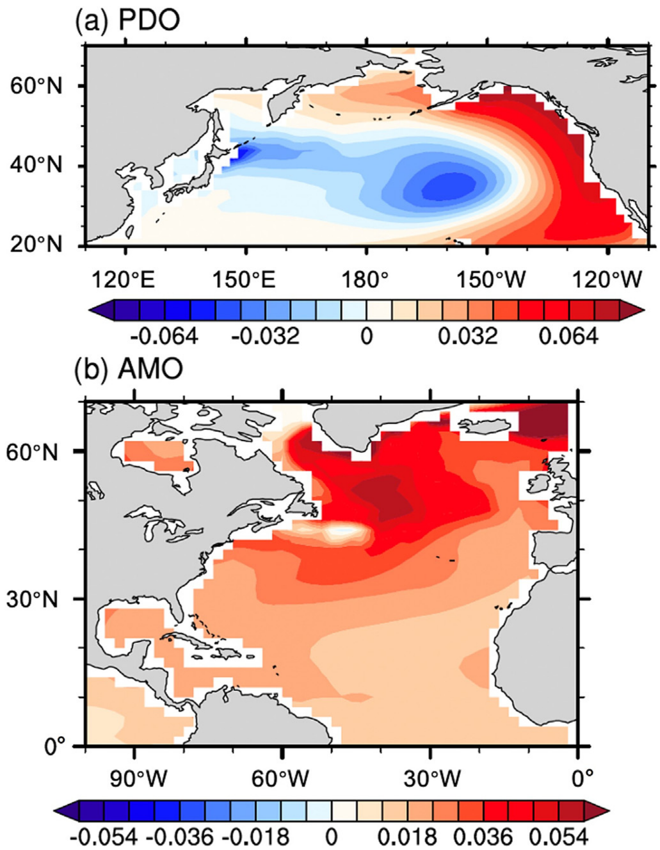

Fig. 2. Spatial patterns of PDV (a) and AMV (b) based on LMR.

These reconstructions have provided comprehensive insights into the historical PDV characteristics with different proxy types and teleconnections around the globe, however, these reconstructions show weak agreement prior to the twentieth century [22,23]. For the preferred time scale, most reconstructions show the existence of multidecadal spectral peaks between 20 to 70 years, but these spectral peaks vary among different reconstructions (Fig. 3a). The strengths of these spectral peaks also change during different periods, showing centennial-scale variations [15]. For the exact PDV phase, there are large discrepancies among the reconstructions prior to the instrumental period, with only significant correlations between two reconstructions both from North American tree-ring data and relatively high correlations between composite reconstructions and individual reconstruction [23].

These inconsistencies among the PDV reconstructions first reflect differences in local climate variable responses to large-scale atmospheric and oceanic variability, due to their limited regional coverage [12], which could be partially improved by using the proxy records from more regions as shown in the two trans-Pacific reconstructions [20,21]. Second, differences in types of proxy records may also contribute to these inconsistencies, due to the potential seasonal growth biases, because the statistical removal of biological growth-related trends in these series may deflate the centennial-scale variability, removing spectral power at the lowest frequencies [12]. Third, these inconsistencies may also arise from time-dependent nonlinearities in PDV and changes in the influence of the tropical climate system over time [22], since the temporal coverages of these reconstructions are different. Furthermore, the shift of dominant PDV preferred time scale from 50–70 years to 25–35 years since 1900 CE [19] is potentially related to global warming, due to strengthened ocean stratification and accelerated Rossy waves based on experiments under the A1B scenario [24]. While, whether the actual CO_2 concentration changes during the CE are significant enough to induce this shift needs to be further investigated using sensitivity experiments. The changes in connection between PDV and TPDV that is mediated by ENSO teleconnections [14] during different typical periods, could also contribute to these inconsistencies.

Therefore, a better understanding of biases and uncertainties in different proxy types, and the dynamics of teleconnections at the proxy sites, will help improve the PDV reconstructions. Meanwhile, investigations on PDV responses to historical external forcings and underlying physical mechanisms through model simulations, could also help reduce the discrepancies among PDV reconstructions. Furthermore, current reconstructions mainly focus on reproducing and extending a single PDV index, while, climate field reconstructions of SST and other circulation variables that might have more stable connections to ecological recorders (e.g., NPGO), may provide more robust alternatives for examining pre-instrumental conditions in the North Pacific [22].

In summary, these multi-proxy PDV reconstructions have improved our understanding of historical PDV evolutions substantially. However, disagreements still exist on the exact phases and preferred time scales of PDV before the instrumental era. Contributions from several uncertainty sources should be first systemically assessed. Then, comparisons with model simulations will help extract the PDV due to internal variability, and also differentiate the different PDV responses to natural and anthropogenic forcings. Furthermore, a deeper understanding of PDV dynamics through sensitivity experiments, such as interactions between tropical and extratropical Pacific and ocean-atmosphere coupling [4], is also crucial to improve both model simulations and proxy reconstructions on historical PDV.

2.3. Atlantic multi-decadal variability (AMV)

The AMV is defined as the primary mode of multidecadal SST variability over the North Atlantic, also termed the "Atlantic Multidecadal Oscillation" or "AMO" [2,6]. For its origin, previous studies found that there is a strong dynamical coupling among North Atlantic Oscillation (NAO), Atlantic meridional overturning circulation (AMOC), and AMV, and their delayed feedbacks within this coupling induce the multidecadal variability over the North Atlantic [25,26]. During the instrumental era, it has been defined in some studies as the leading low-frequency mode after removal of the linear trend or global mean temperature, because it shares similar trends and multidecadal variability with the Northern Hemisphere temperature [6]. However, Steinman et al [13] demonstrate that such procedures result in biased estimates of internal variability owing to residual forced trends that such procedures fail to remove. Recognizing that "AMV" defined in these ways contains both internal and forced variability, the pattern during the historical period, shows positive loadings at mid- to high-latitude North Atlantic (Fig. 2b). Mann et al. [2] show that the apparent positive values during the middle 20th century and negative values during the late 20th century are largely attributed to decreased aerosol radiative forcing following the passage of the clean air acts in the 1970s and 1980s.

During the pre-industrial CE, similar to PDV, AMV reconstructions have been attempted based on tree-ring records around the North Atlantic region [27,28], and global multiple proxy records [7]. Besides these reconstructions based on terrestrial proxy, a new AMV reconstruction extending to the past 3 millennia at annual resolution, is reconstructed using varved sediments from Ellesmere Island, which overcomes the typical low-resolution drawback of marine records [29].

These AMV reconstructions generally share similar multidecadal behavior, with significant correlations, although there are

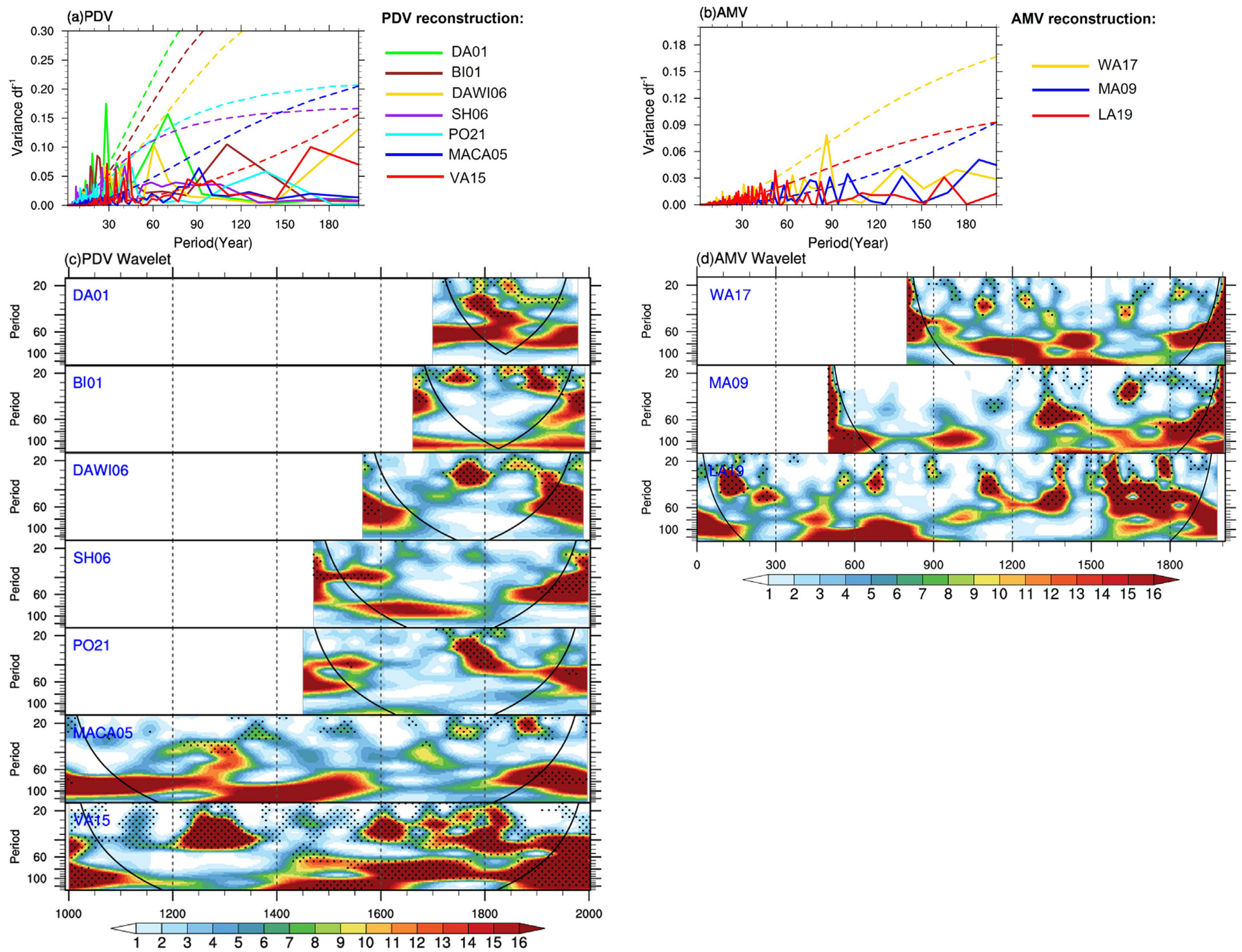

Fig. 3. Power spectral (a, b) and wavelet analyses (c, d) for the PDV (a, c) and AMV (b, d) reconstructions. All reconstructed PDV and AMV indices are normalized to unit variance for comparison.

still some inconsistencies on shorter-scale variability (Fig. 1c). They also significantly correlate to other local temperature reconstructions and isotope records over the North Atlantic that can also be used as fingerprints of AMV [29]. These AMV reconstructions also show a prolonged AMV negative phase during LIA. However, this AMV negative phase may simply reflect the corresponding regime of lowered global mean temperature as commented on earlier. For the preferred time scale, all reconstructions show existence of multidecadal spectral peaks between 60 to 100 years as explained by the delayed oscillator model describing the NAO-AMOC-AMV dynamical coupling processes [25,26], but the dominant spectral peaks vary slightly (Fig. 3b). However, the AMV reconstructions with updated tree-ring data has stronger and more persistent multidecadal variability before the 16th century compared to the previous two reconstructions, potentially due to differences in reconstruction methods or precise composition of the proxy network [28].

Another potential issue is how these reconstructed AMV reflect the true multidecadal variability of northern Atlantic SST, rather than the global mean surface temperature. For instance, when the component regressed on the global-scale signal is removed, there is essentially not much AMV signal in LMR, in contrast to the pronounced multidecadal variations exhibited in the instrumental AMV index [6]. Wang et al. [28] also found that explosive volcanic and solar forcing are responsible for only a modest (roughly 30%) share of AMV variance. However, Mann et al. [30] show that the procedures typically used in these past analyses to define AMV fail to isolate the internal variability component in the process of forced variability. They show that the existence of apparent 50–70-year oscillatory variability during the pre-industrial era is an artifact of volcanic forcing, which happens to project heavily onto this frequency band during the pre-industrial CE [30]. Therefore, one might instead, for example, consider the residual series resulting from the removal of the global mean surface temperature, though this procedure is subject to potential biases as noted by Steinman et al. [13].

In summary, besides the AMV defined from global temperature reconstructions, there are fewer specific AMV reconstructions than PDV. However, due to the high correlations with the global or northern hemisphere mean temperature [28], these AMV reconstructions include both the global responses to external forcings and intrinsic variability of the northern Atlantic. Large ensemble simulations from multiple models and suitable statistical methods [13] are needed to differentiate these forced components and intrinsic variability. Furthermore, the disagreement on the stationarity of the multidecadal variability during the present warming period and LIA [27,29], also indicates the necessity for future study on AMV responses to anthropogenic and natural forcings.

2.4. Atlantic meridional overturning circulation (AMOC)

During the instrumental period, the AMOC has been observed directly in the instrumental record only since 2004, which severely limits the understanding of its long-term variability. As a result, even the AMOC variability in the instrument period has to be studied using fingerprints, derived from temperature and salinity observations. A recent study evaluated five AMOC representative indicators, including one atmospheric index based on accumulated atmospheric forcing and four oceanographic indices using surface and subsurface oceanographic variables in the North Atlantic Ocean. All these AMOC indicators show a weakening trend as found in RAPID measurement, with the atmospheric index showing the best agreement with the observed low-frequency AMOC variations since 2004 [31]. These five AMOC indicators have also been used to investigate the connections between AMOC and Northern Hemisphere precipitation on the multidecadal scale [32], and multidecadal seesaw pattern in tropical cyclone activity [33]. It is found that the atmospheric index shows a leading role in depicting these connections, and could serve as a predictor for decadal predictions of North Hemisphere precipitation and North Atlantic tropical cyclones [32,33]. These fingerprints tend to suggest a strong AMOC decreasing trend starting in the 19th century, followed by a rapid decline in the middle 20th century, leading to the weakest state of the AMOC occurring in recent decades [34]. Zhu and Liu [35] found that salinity in the South Atlantic serves as a fingerprint of AMOC intensity, and recent salinity pile-up in the South Atlantic indicates AMOC weakening through the salinity divergence reduction. Moreover, there is a likely accelerated AMOC weakening since the 1980s, which is absent in the classic warming hole fingerprint that is contaminated by interdecadal variability [35]. However, some studies based on observation and satellite data argue that the AMOC has remained stable since the 1990s, implying a decoupling between the AMOC and ocean interior property fields [36]. Therefore, even though these fingerprints suggest a decline of AMOC, the detailed behavior of AMOC remains highly uncertain.

Proxy reconstructions during the pre-industrial CE provide an opportunity to investigate its variability and mechanisms with a longer-term perspective. According to reconstructed AMOC derived from different proxy types, e.g., isotopes and species abundance from foraminifera [37], mean grain sizes [38], and SST fingerprints [39], there is strong AMOC during the MCA, while weaker AMOC during the LIA (Fig. 1d). These AMOC reconstructions agree on the declining trend through the pre-industrial CE, but differences on multidecadal or shorter scale variability exist. Furthermore, as fingerprints, these reconstructions cannot provide an exact magnitude of historical AMOC variations, posing a necessity for quantitative AMOC reconstructions in future studies.

Model simulations have provided insights into mechanisms behind these centennial scale AMOC variations found in proxy records during the pre-industrial CE. Some studies argue that anomalous atmospheric circulation, such as regime shift of NAO [40], is also considered to play a significant role in triggering AMOC decline from MCA to LIA. On the aspect of external forcings, based on recent AMV and AMOC reconstructions, it is found that the LIA was associated with the weakening of the subpolar gyre due to an exceptional intrusion of warm Atlantic water into the Nordic Seas linked to persistent atmospheric blocking over North Atlantic induced by unusually high solar activity [41]. Meanwhile, under anthropogenic warming, the weakened AMOC can also decelerate the North Atlantic subpolar gyre through the anticyclonic surface wind anomalies over the subpolar North Atlantic [42]. However, there are some discrepancies between proxy reconstructions and model simulations regarding the onset timing and magnitude of this AMOC weakening at the end of LIA, indicating the necessity to improve understanding of the evidence of freshwater fluxes during this period, the sensitivity of AMOC to freshwater forcing, etc. [39].

In summary, although available AMOC reconstructions show agreements on the centennial variations during the CE, their low resolution makes it still challenging to investigate the decadal to multi-decadal variability of AMOC. Furthermore, all these AMOC reconstructions are fingerprints, which can only represent the trends and variations, instead of the magnitudes of these trends and variations in true AMOC transport.

2.5. Decadal modulation on interannual climate changes

2.5.1. Decadal to multi-decadal modulation of El Niño-southern oscillation (ENSO) variability and teleconnections

As the dominant mode of interannual variability of the earth's climate system, ENSO and the associated teleconnections exhibit considerable decadal to multidecadal scale variations in amplitude and frequency (Fig. 1e). A continuous annually resolved ENSO records during the past millennium, reconstructed using tree-rings data around North America, shows a quasi-regular interdecadal modulation of ENSO amplitude, with anomalously high ENSO activity in the late 20th century than over the past seven centuries, suggestive of a possible strengthening response to human-caused warming [43].

Low-frequency modulation of ENSO during the pre-instrumental CE may be a result of changing solar and volcanic radiative forcing, as noted by Mann et al [9]. Some work has speculated that PDV and AMV modulate ENSO variability including the frequency of El Niño and La Niña events [44], but as noted earlier, much AMV variability has actually been tied to radiative forcing changes in recent work [3]. During the positive phase of PDV (or its tropical expression TPDV), El Niño events tend to occur more frequently than La Niña events [14]. Regarding the role of AMV, it has been speculated that it modulates multidecadal ENSO variance and also seasonal stability of ENSO by changing the seasonal cycle with a positive AMV phase increasing trade wind strength and enhancing the equatorial Pacific cold tongue [45]. On the magnitude aspect, proxy reconstructions and model simulations indicate that a positive AMV enhances the zonal sea surface temperature gradient in the central Pacific, which strengthens zonal advective feedback and favors extreme and central Pacific (CP) El Niño development, inducing decadal variations of El Niño types [46]. However, these detailed mechanisms are primarily discussed within the instrumental era, with little investigation during the CE, leaving an opportunity to investigate the decadal to multidecadal ENSO modulations in longer periods with more external forcing.

On the aspect of ENSO teleconnection, the decadal to interdecadal modulation of ENSO variability also shows substantial modulation of ENSO teleconnections across the pan-Pacific regions for the past seven centuries, with reduced teleconnection strength during the Maunder minimum [43]. In response to the AMV and PDV, there is a robust positive correlation between ENSO and western North Pacific anticyclone and spring precipitation over southern China, a.k.a. atmospheric combination mode, during a negative AMV phase but not during a positive phase, because weaker ENSO magnitude and westward-shift SSTA pattern during a positive AMV phase [47]. The ENSO-EASM relationship has been argued to be stronger in the warm phase of the IPO, attributing to IPO modulation on amplitudes of the ENSO variability and El Niño and La Niña frequency asymmetry [48]. Besides the AMV and PDV, the multidecadal variability of the NAO may impact North Tropical Atlantic (NTA) SSTA and, thereby, ENSO, through strengthening of the boreal spring mean precipitation over the equatorial Atlantic and enhancing the persistence of NTA SSTA [49]. It has been argued that high solar irradiance weakens the ENSO-EASM correlation, but strengthens the ENSO-SASM correlation, through changes in the Western Pacific Subtropical High and the amplitude of ENSO events, respectively [50].

2.5.2. Decadal to multi-decadal modulation of South Asian summer monsoon (SASM) changes

Decadal climate variability has also been observed clearly in the CE over land regions, notably for the monsoon systems. Over the Asian monsoon region, besides the proxy records, such as tree-rings and speleothem δ^{18}O, etc., there are several gridded data sets reconstructions extending back through the CE, including dry-wet index [51], warm season precipitation [52,53], and Palmer drought sensitivity index (PDSI) [54], which provide unique opportunities to investigate the decadal-scale variability of Asian monsoon and sub-monsoons.

For the SASM (Fig. 1f), observations underscore a drying trend in the SASM precipitation during the period 1950–2002, which is also recorded in the Indian speleothem δ^{18}O and tree-ring width reconstructions [55,56]. However, some studies argue that this drying trend has not exceeded the envelope of SASM variability witnessed in the proxy records over the last millennium [55]. As for the spatial characteristic, the reconstructed SASM precipitation variability during the CE also shows obvious regional differences. For instance, high-resolution speleothem δ^{18}O records in central and northeastern India exhibit opposing precipitation behavior on centennial time scales, with enhanced east-west dipole pattern during AD 1700–2007 and a weakened dipole pattern from 1400 and 1700 [55].

On the aspect of preferred time scale, during the period 1470–2013, the reconstructed all-Asian rainfall shows significant low-frequency time scales on decadal (8–10 years), quasi-bi-decadal (22 years), and multidecadal (50–54 years), with a remarkable change of leading frequency from multidecadal to decadal after 1700 [53]. As for the SASM, insights from the speleothem δ^{18}O records during the last two millennia indicate the presence of significant 60–80 and 15–30-year time scales [57], which are associated with AMV through changing the meridional temperature gradient between the Tibetan Plateau and the tropical Indian Ocean [58]. However, these preferred time scales exhibit non-stationary behavior during the CE, and the 60–80-year variability stands out during specific time intervals, notably from 300 to 500, 1500 to 1700, and 1850 to 2000.

When comparing proxy reconstructions and model simulations, Fan et al. [59] found that there are limited agreements between model-based SASM and proxy reconstructions, as well as among proxy reconstructions themselves, during the last millennium, indicating that external forcing might dominate multidecadal variability of SASM. In response to external forcings, Fan et al. [59] found that solar-forced signal in long-term SASM behavior appears to be undetectable, probably due to weak radiative forcing compared with intrinsic climate noise, while explosive volcanism induces significant SASM decreases. However, proxy reconstructions show a significant positive correlation with solar forcing, and this may indicate the lack of dynamic tropical Pacific ocean-atmosphere response to radiative forcing in the simulations. Furthermore, whether the decoupling between SASM and ENSO in recent decades is caused by aerosols and volcanic eruptions [60] could also be investigated in the CE.

2.5.3. Decadal to multi-decadal modulation of East Asian summer monsoon (EASM) changes

During the instrumental era, the EASM has exhibited a weakening trend since the late 1970s, followed by a recovery trend in the 1990s, resulting the decadal-scale droughts over northern China [61]. These decadal EASM changes associated with shifts between dipole pattern and tripolar pattern of summer precipitation over eastern China [62], align with the natural variability observed over the past five hundred years, as evidenced by reconstructions based on tree-rings, speleothems, and historical documentary data [63] (Fig. 1g). After extracting the interdecadal to centennial components, proxy data reveal a long-term wetting trend in eastern China prior to the 18th century, transitioning into a prolonged drying trend thereafter [51,52].

Associated with weak EASM, northern China witnessed five decadal-scale megadroughts during the last millennium, occurring in the periods of 1146–1155, 1240–1249, 1483–1492, 1578–1587, and 1634–1643, respectively [64]. Concurrently, analogous dry conditions manifested in India and Pakistan [54], indicating synchronous weak SASM events. When considering EASM and SASM together, Cook et al. [54] also identified four severe megadroughts over the whole monsoon Asia associated with Asian monsoon failure, i.e., Ming Dynasty Drought (1638–1641), Strange Parallels Drought (1756–1768), East India Drought (1790–1796), and The Great Drought (1876–1878) during the last millennium. The relationship between all-Asian rainfall and mega-ENSO is persistently significant except from 1820 to around 1900, while the relationship between all-Asian rainfall and AMV is nonstationary [53].

Similar decadal scale EASM variability and associated megadrought events are also evident in model simulations during the CE [65]. However, direct phase comparisons of decadal monsoon variability between long-term proxy reconstructions and model simulations are limited by internal variability in the model simulations, as well as the uncertainties among different reconstructions and model dynamics. Only decadal variability caused by external forcings, such as volcanic eruptions and solar radiation, can be partially compared [65]. Nevertheless, there are still considerable uncertainties on magnitudes and durations of these variabilities, because responses to the same external forcing differ among models and proxy records. So, this highlights the importance of sensitivity experiments in exploring the physical mechanisms behind these decadal monsoon variabilities, as discussed in the following sections.

In summary, decadal variations of ENSO, SASM, and EASM intensities are closely associated with PDV and AMV phases and magnitudes, such that they share the same uncertainties with PDV and AMV reconstructions, such as the mismatches of specific decadal phases and shifts of preferred time scales. Furthermore, the ENSO reconstructions are based on the assumed stationarity of teleconnections between local proxy records and SSTA, so the centennial variations of teleconnections may impact the reconstructed ENSO magnitudes. Another potential caveat is that they rely on extratropical teleconnections of ENSO rather than direct measures of tropical Pacific ocean-atmosphere behavior [43]. The physical mechanisms driving these changes in decadal ENSO variability, such as changes in SST over the eastern Pacific or zonal SST gradient in the equatorial Pacific, may also be different. The SASM and EASM reconstructions, most of which are related to regional precipitation variations (e.g., historical documents and tree-rings) with more complex internal variability and responses to external forcings than the temperature, have extra spatial heterogeneity but less temporal uncertainty than those reconstructions representing monsoon circulations (e.g., speleothem) [66]. Therefore, better reconstructions require detailed investigations of regional internal variability and responses to external forcings, and corresponding mechanisms, with the help of model simulations.

3. Mechanisms for decadal climate variability

Decadal variability can be caused by processes internal to the coupled ocean-atmosphere system, as well as being externally forced. The mechanism of internal decadal variability has been studied extensively in the context of present climate variability [4,12]. Despite intensive studies, the mechanisms of internal decadal climate variability remain uncertain. As the null hypothesis, decadal variability modes have been suggested to be interpreted within the framework of stochastic climate model [4,5]. The impact of stochastic forcing from weather noise is accumulated by the ocean due to its long-term memory, while oceanic processes and ocean-atmosphere interactions also potentially play significant roles [4]. Much of the decadal variability has been attributed to external forcings, notably volcanic eruptions, solar variability, and anthropogenic forcings [2,3]. Since the mechanisms of internal decadal variability have been reviewed extensively in previous studies [4–6], we focus here on the role of external forcings.

3.1. Influences from external forcings

Volcanic eruptions and solar radiation have been found to exert significant influences on decadal-scale global and regional temperature changes (Fig. 4a). Based on proxy reconstructions and model simulations, Wang et al. [67] found that strong tropical volcanic eruptions and variations in total solar irradiance play an important role in regulating North Pacific decadal variability. Based on a network of annually resolved terrestrial proxy records from the circum-North Atlantic region, the reconstructed AMV for the period 800–2010 show that large volcanic eruptions and solar irradiance minima induce cool phases of AMV and collectively explain about 30% of AMV variance [28]. Liu W et al. [68] also found bidecadal temperature anomalies over the Tibetan Plateau and the Arctic in response to the 1450s volcanic eruptions in both proxy records and model simulations.

On the aspect of direct influences from volcanic eruptions and solar radiation on precipitation over the Northern Hemisphere, a prevailing perspective is that substantial volcanic eruptions suppress the Northern Hemisphere summer monsoon precipitation on interannual to decadal scales, through reducing in the summer land-sea thermal contrast [69,70] (Fig. 4b). Furthermore, the diminished atmospheric moisture content and soil moisture feedback perpetuate the decadal decline in EASM precipitation [71]. The combined effect of internal variability and volcanic forcing can aggravate decadal EASM weakening and megadroughts over eastern China [65]. For instance, the late Ming Dynasty megadrought (1637–1643) was probably triggered by internal variability, and intensified and prolonged by the eruption of the Parker volcano in 1641 [70,71]. For the indirect influences from consecutive volcanic eruptions, it is found that there is ~60-year preferred time scale for PDV and AMV during the LIA in the volcanic eruption sensitivity experiment, consistent with the proxy reconstructions [72] (Fig. 4c, d). Furthermore, consecutive volcanic eruptions (Fig. 4e) could also trigger a multidecadal weakening of EASM and corresponding precipitation decreases over eastern China by inducing negative AMV phases [73].

On the aspect of influences from solar radiation (Fig. 4f) on precipitation over eastern China, Xue et al. [74] compared the frequencies of weak EASM events between MCA and LIA, and found that the frequency is significantly higher during LIA because the nonlinear response of the precipitation to the large-scale atmospheric circulation patterns associated with positive PDV phases. It is found that the precipitation differences between positive and negative PDV phases increase with solar radiation intensity due to the large-scale circulation changes [75]. It is also found that the frequency of large Meiyu events increases during periods with strong solar radiation, indicating that solar radiation modulates these interannual events [76].

On the aspect of anthropogenic forcing, it is found that the leading pattern of decadal EASM precipitation changes shifts from a dipole pattern to a tripolar pattern after 1750 in sensitivity experiments, because the land-use and land-cover change (LUCC) increases the occurrences of different PDV and AMV phases and alters the Rossby wave train and circulation patterns over eastern China [62]. The warming of increasing greenhouse gas concentrations (GHG) intensified droughts over northern China associated with EASM weakening in recent decades through the increased evaporation, and this EASM weakening may be triggered by the PDV and AMV phase changes induced by anthropogenic aerosols [77] (Fig. 4g, h). Meanwhile, Cheng et al. [78] found that, in response to enhanced global warming, the multidecadal variability of AMOC becomes weaker and shorter, with major periods from ~50 years to ~20 years and amplitude reduced by ~60%. In these changes of AMOC multidecadal variability, the mean flow effects, in the form of eastward mean zonal advection and westward geostrophic self-advection, play an important role through increasing the speed of Rossby waves and in turn the AMOC variability in a continuously stratified ocean [79].

In summary, the direct influences on global and regional decal climate variability from external forcings are mainly achieved through changing surface energy budgets, such as direct changes of shortwave radiation and longwave radiations arriving at the ground, and surface albedo. The indirect influences are achieved through changing PDV and AMV phases or frequencies, either single-phase changes due to volcanic eruptions or frequency changes in response to background changes due to other forcings. With this improved understanding of the mechanisms behind decadal variability, some statistical methods such as emergent constraint, could be applied to model simulations to reduce the uncertainties due to model internal variability and improve decadal predictions [80]. Specifically, these accurate predictions will help to meet the huge challenges of drought risks in northern China and prepare the corresponding adaptation strategies.

3.2. Internal variability vs. External forcing

3.2.1. Different contributions to global temperature variations

It has remained controversial if decadal variability in the instrumental period is caused predominantly by internal variability or external forcings [81,82]. The CE provides a unique opportunity to compare the influences from internal variability and external forcings, such as volcanic eruptions, due to the much larger sample size than the instrumental period.

On the aspect of decadal global temperature changes, in comparison of observations and simulations from an energy balance climate model, Crowley [83] found that as much as 41% to 64% of pre-1850 decadal variability in global mean temperature is caused by changes in solar irradiance and volcanic eruptions. Based on observations as well as forced and control model simulations, Mann et al. [2] found that the multidecadal scale variability in global mean surface temperature observation reflects the response of the climate system to both anthropogenic and natural forcings rather than any intrinsic internal oscillations. While it remains unclear that components due to internal variability could be generated through the removal of forced components. Crowley [83] found that removal of the forced response from reconstructed temperature time series yields residuals that show similar variability to those in control runs of coupled models, thereby lending support to the models' value as estimates of low-frequency variability in the climate system. But Mann et al. [84] found that regression-based methods of removing the forced component from proxy reconstructions will, fail to yield accurate estimates and incorrectly attribute unresolved forced features to internal variability. Notably, this relative contribution from external forcing is smaller in the multi-decadal scale local climate variability. In general, local climate variability is affected more by internal variability, whereas the global mean could maximize the impact of external forcing

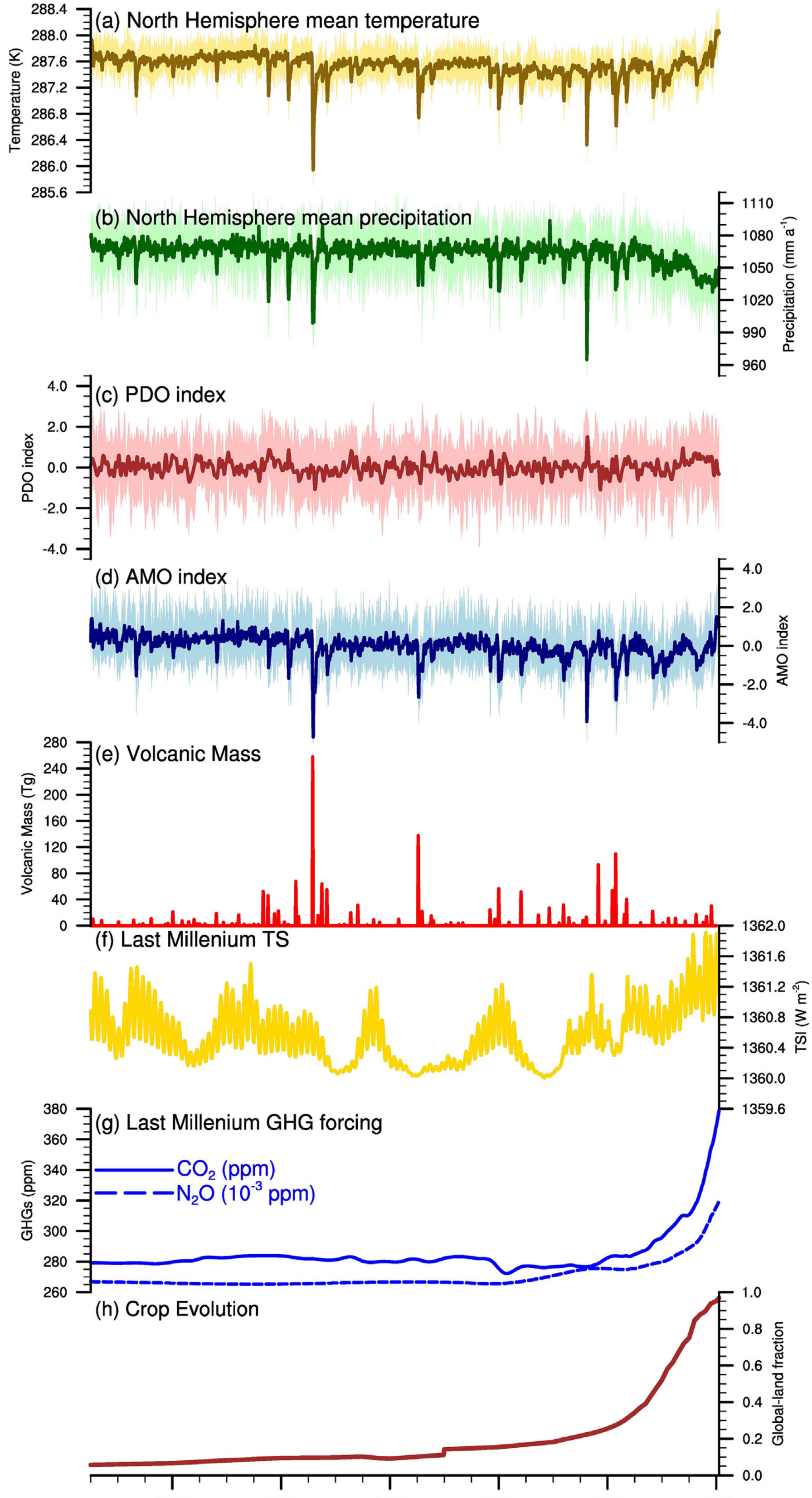

Fig. 4. Simulated northern hemisphere mean temperature changes (a), precipitation changes (b), PDV (c), AMV (d), volcanic aerosol forcing (e), TSI forcing (f), GHG concentrations forcing (g), crop extent forcing (h) during the period 850–2005 from CESM-LME all-forcing experiments.

because internal variability tends to generate substantial spatial variability and therefore their signal is suppressed in the global mean.

Moreover, based on reconstructed GMST over the past 2000 years, PAGES 2k Consortium found that a substantial portion of pre-industrial GMST variability at multidecadal timescales is attributed to volcanic aerosol forcing, because of the synchronous multidecadal temperature fluctuations observed among proxy records and between CMIP fully forced simulations [8]. However, there were no globally synchronous multidecadal warm or cold intervals [11]. This lack of spatiotemporal coherence on warm and cold epochs indicates that pre-industrial forcings were not sufficient to produce globally synchronous extreme temperatures at multidecadal and centennial timescales [11].

3.2.2. Different contributions to PDV and AMV

On the aspect of decadal variability, some studies based on instrumental observations and model simulations indicate that PDV and AMV reflect the responses of North Pacific and North Atlantic SST to stochastic atmospheric forcing [5] or external radiative forcing [67,85]. But some studies argue that this decadal SSTA variability is dominated by internal variability, because when the signal regressed on global mean SST is removed, the externally forced AMV in a multi-model ensemble exhibits a negative spatial correlation with the observed AMV [86]. This poses a challenge on how to properly distinguish forced AMV signals from internal variability, and the necessity of investigations using the longer-term proxy records and model simulations [13,84].

Meanwhile, during the CE, some studies also found that strong volcanic eruptions were followed by decadal-scale positive responses of the AMOC, indicating the potential influences on the whole North Atlantic climate system [87]. Therefore, a recent study examined the influences of volcanic eruptions on North Atlantic SSTA and thermocline together, and revealed that strong volcanic eruptions could reset SSTA and subsurface temperature anomalies, but could only modulate the AMOC, indicating external forcings could influence the AMV both directly and indirectly through internal ocean circulation [88].

Moreover, the global scale multidecadal variability of SST could be driven by the AMV through atmospheric teleconnections and atmosphere-ocean coupling processes. Wang et al. [28] also conclude that the apparent link between AMV and regional to hemispheric climate does not arise solely from a common response to external drivers, and may instead reflect dynamic processes. A recent study indicates that the relationship between cross-equatorial gradient in tropical Atlantic SSTs and radiative perturbations is obscured in the ensemble of CMIP6 simulations, because models overestimate long-term trends of warming in the NH relative to the Southern Hemisphere [81].

Another important aspect of decadal variability is the interaction between PDV and AMV. This interaction between PDV and AMV regulates the regional temperature and precipitation through a modulation of the inter-basin Walker circulation and the associated Rossby wave train into northern extratropics [89]. Usually, there are two pathways, i.e., the extratropical pathway and tropical pathway [6]. The extratropical pathway is through the changes of mid-latitude winter storm track and shift of KOE [90] (Fig. 5a) or North Pacific wind-evaporation-SST effect and SST-sea level pressure-cloud-longwave radiation positive effect [91] (Fig. 5b). The tropical pathway is through the changes of the Walker circulation and precipitation anomalies over the whole tropical belt [44], interhemispheric asymmetry of net moist static energy input into the atmosphere [92], and easterly wind anomalies over the Indo-western Pacific [93], etc.

Based on pacemaker experiments, Meehl et al. [94] found that there tends to be a weak opposite-sign SST response in the tropical Pacific when observed SSTs are specified in the Atlantic (Fig. 5c), while there is a weak same-sign SST response in the tropical Atlantic when observed SSTs are specified in the tropical Pacific, through Walker circulation along with contribution from midlatitude teleconnections for the Atlantic response to the Pacific (Fig. 5d). While, these interactive influences do not drive an oscillation. Among the factors influencing the interactions, it is found that this interaction depends on the phase relationship of PDV and AMV [95], and aerosols may also impact this interaction by driving the tropical North Atlantic [94].

Similar to the other decadal problems, the short temporal coverage of observational data limits detailed analyses about this interaction. It is important to investigate this topic within the last two millennia. However, the uncertainty within reconstructed PDV and AMV phases further limits these analyses using proxy reconstructions.

In summary, despite substantial progress so far, the relative contributions to decadal variability from internal variability and external forcings remain difficult to quantify, especially for regional or local climate variability. This is caused by the limited ability of attribution methods, inconsistencies among proxy reconstructions, and model biases. Furthermore, the complex dynamics of PDV and AMV, as well as their mutual interaction and their responses to external forcings, also contribute to this issue. Therefore, improved methods to differentiate internal and external components within proxy reconstructions, and a better understanding of the dynamics of internal variability and responses to external forcings through sensitivity experiments, are crucial to resolve this issue in the future.

4. Summary and Perspective

With support from PAGES2k Network, CLIVAR DCVP, CMIP6 DCPP, and WCRP, recent advances in proxy reconstructions and model simulations have substantially improved our understanding on the characteristics and mechanisms of decadal climate variability during the pre-industrial CE. On the aspect of characteristics, multiple proxy reconstructions and model simulations show agreements on the phases of multidecadal GMST variability, PDV, and AMV, induced by external forcings, and relatively weaker agreements on the amplitudes. However, for the unforced multidecadal climate variability, there are disagreements on the exact phases and preferred time scales, which are potentially due to the different types, regional coverage, and temporal coverage of proxy records, and the time-dependent nonlinearities of decadal climate variability. The decadal variability of ENSO, SASM, and EASM have similar uncertainties with PDV and AMV, because they are largely modulated by PDV and AMV. While, examining decadal phases and amplitudes of AMOC is more challenging, due to the low resolutions and fingerprint natures of the AMOC reconstructions.

On the aspect of mechanisms, the influences of global and regional decal climate variability from external forcings, i.e., volcanic eruptions, solar radiation, LUCC, GHGs, and anthropogenic aerosols, have been systematically investigated. These influences from external forcings include direct influences through changing surface energy budget changes, and indirect influences through changing PDV and AMV phases or frequencies. However, the relative contributions from internal variability and external forcings are still difficult to quantify, due to the inabilities of attribution methods, proxy reconstructions, and model simulations. Furthermore, the responses of PDV and AMV to external forcings and the corresponding dynamics need to be further investigated through sensitivity experiments.

Besides these progresses, however, there are still many challenges remaining unresolved as discussed below, which should be addressed in future studies.

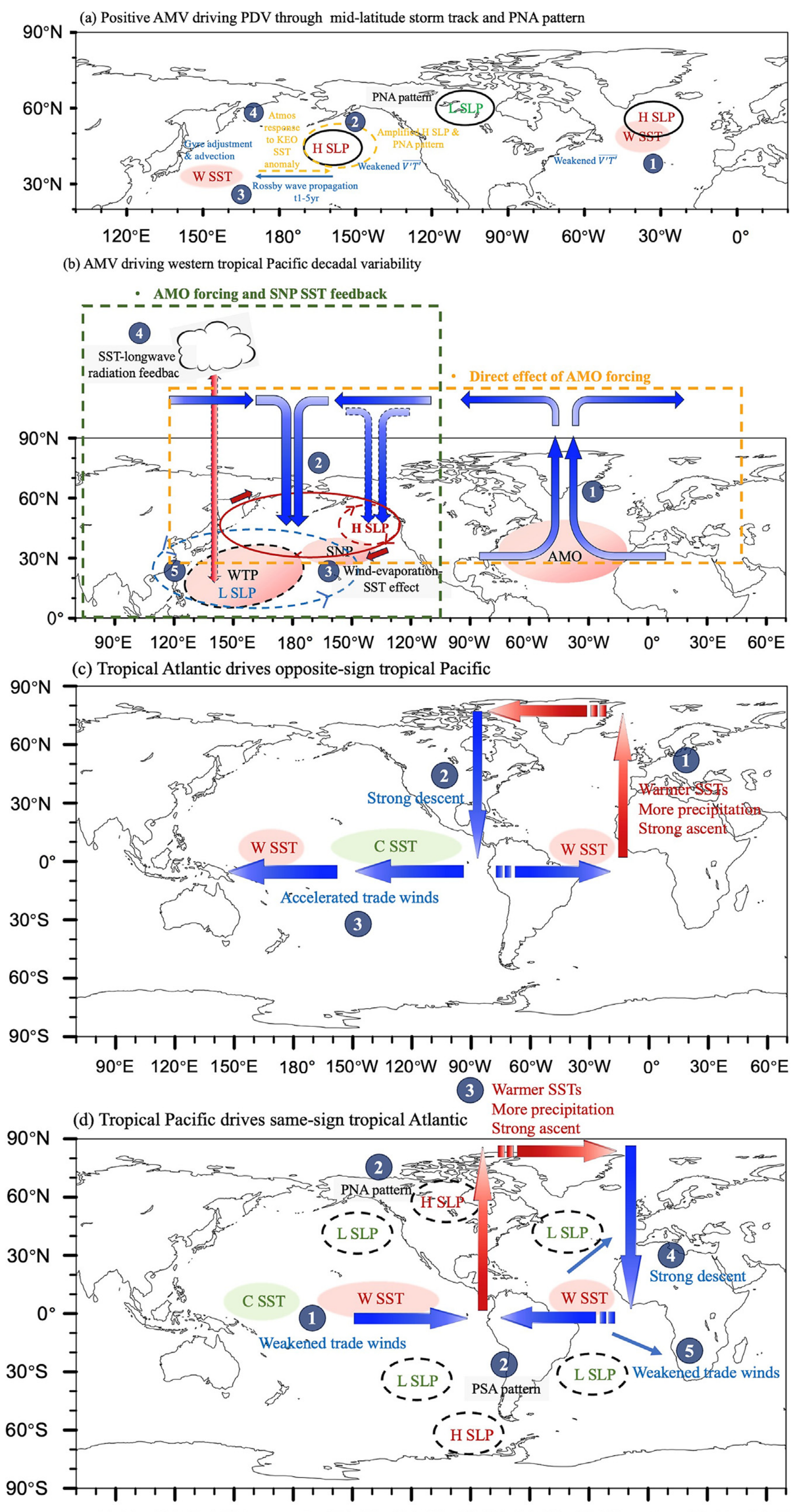

Fig. 5. Schematic diagram for the PDV and AMV interactions. (a) Positive AMV driving PDV through the northward mid-latitude storm track and anomalous Pacific/North American (PNA) pattern, and reinforced by oceanic dynamics and positive air-sea feedback over the North Pacific. (a) Reprinted from Ref. [90]. Copyright (2007) American Geophysical Union. (b) AMV driving western tropical Pacific decadal variability through wind-evaporation-SST effect and SST-longwave radiation feedback. (b) Reprinted from Ref. [91]. Copyright (2017) Springer Nature. (c) Positive AMV contributing to opposite-sign SST response of negative PDV in the tropical Pacific mainly through the tropical Walker circulation (d) Same as (c) except for positive PDV in the tropical Pacific contributing to same-sign AMV in tropical Atlantic with contributions from the tropical Walker circulation as well as extratropical PNA teleconnections. (c) and (d) Reprinted from Ref. [94]. Copyright (2021) Springer Nature.

4.1. Understanding the discrepancies of decadal variability among different proxy reconstructions

Although obvious decadal variability exists within the proxy reconstructions, the preferred time scales are different ranging from 20 years to 80 years among different data sets of proxy reconstructions. For example, for PDV reconstructions, decadal to multi-decadal variability exists in the power spectral of all the proxy reconstructions, but with different dominant peaks, such as the 20 years and 70 years [15] (Fig. 3a). However, these multi-decadal spectral peaks shown in the PDV reconstructions are not significant in the power spectral of observed data sets [12]. For AMV, all reconstructions exhibit similar multi-decadal variability, but with slightly different preferred time scales, as 50–70 years in Mann et al. [30], 64–88 years in Wang et al. [28], and 42–83 years in Lapointe et al. [29] (Fig. 3b). These inconsistent multi-decadal variabilities in proxy records may be related to the differences in the length of proxy records, because Lapointe et al. [29] found the AMV shows enhanced multi-decadal variability since the late 16th century. In model simulations, it is also found that the 50–70-year time scales of PDV and AMV are induced by volcanic eruptions during LIA, while the 20–40-year time scales are due to internal variability before LIA [72]. The wavelet analyses of PDV and AMV (Fig. 3c, d) confirm the temporal evolutions of these preferred time scales, with the enhanced multi-decadal variability during the periods with strong volcanic eruptions. So, the covering periods of proxy reconstructions may explain the differences in preferred time scales, due to the centennial-scale variations of preferred time scales due to volcanic eruptions and solar radiations. On the other aspect, the resolutions may also contribute to this difference. Therefore, these significant discrepancies among reconstructions require future detailed studies.

Furthermore, the phases of decadal variability among different proxy reconstructions do not match, either, even in response to the strong volcanic eruptions. These different phases may relate to the inconsistent teleconnections between the large-scale decadal variability and local climate variables represented by different types of proxy records [18]. Even for the same type of proxy, the unsynchronous teleconnection changes over different regions may also result in different phases. Furthermore, some technique issues, such as potential seasonal biases, biological growth rates in tree-ring data, dating errors, etc., may also contribute to these phase uncertainties.

PAGES 2k Network has been targeted to reduce uncertainties in paleoclimatic archives and to identify the extent of agreement between reconstructions and model simulations [8]. This requires an improved understanding of the physical mechanisms of teleconnections between decadal variability and regional climate variables under different climatic backgrounds, with the help of model simulations. Moreover, within specific studies, applications using multiple types of proxy records are necessary because the inherent biases from individual proxy types could be partially canceled out.

The PDV and AMV reconstructions are always defined as the raw SST reconstructions with mean states kept, which results in persistent positive or negative phases of these variabilities [15,18]. To reconstruct the exact variability in the future, the SST mean states during typical warm and cold periods should be removed first, as the definitions with global warming fingerprint removed during the present warming period [6].

4.2. Model-data comparison on decadal variability during the CE

Quantifying the responses, feedback, and uncertainties intrinsic to the changing climate system on decadal timescale is a major scientific objective of the WCRP Strategic Plan 2019–2028. However, due to the inability of models to reproduce the exact phases of internal variability, significant differences may appear when comparing model simulations with proxy reconstructions, limiting our confidence in achieving this scientific objective. Additionally, in response to the external forcing, especially the volcanic eruptions, model simulations tend to generate larger responses than proxy records, with higher spatial coherency. This indicates that the models may potentially underestimate the magnitude of internal variability, or chemical and biological processes induce uncertainties in proxy records due to the non-climatic noise [96].

To reduce the discrepancies between model simulations and proxy reconstructions, the potential biases and limitations in both proxy reconstructions and simulations due to internal variability and responses to external forcings, should be systematically assessed and compared first. Improved climatic interpretation of proxy records [97] could contribute to the understanding of decadal climate variability and mechanisms. Reducing dating uncertainties in proxy reconstructions could also help improve the comparison between model simulations and proxy reconstructions. Moreover, comparisons on the large-scale climatic modes, rather than single index or regional variations, will be more meaningful. Reconstructions of these large-scale climate modes typically reply on proxy networks, which could minimize biases arising from different proxy types, and also capture stable imprints even if the teleconnection patterns change through time [98].

Then, data assimilation, employing the useful information in proxy records and physical constraints in the model, provides an opportunity to reconstruct a more reliable decadal-scale paleo-climate during the CE. For example, global temperature and drought index during the CE have been reconstructed through DA, e.g., the LMR and PHYDA [9,10]. However, further paleo-climate DA for hydroclimate and systematic evaluations of uncertainties, from global to regional scales, are still limited. In the future, with the improvement of both proxy reconstruction and model simulations, data assimilation can also be used to combine data and model optimally to reconstruct atmospheric and oceanic circulations beyond the surface variables, such as AMOC.

While, in the paleo-climate DA procedure, besides the potential caveats in proxy reconstructions and model simulations, the assumed linear relationships between proxy records and climate variables (a.k.a., proxy system model, PSM), also limit the accuracy of reconstructed decadal climate through DA. More accurate PSMs, especially the PSMs describing nonlinear relationships between different proxy types (such as pollen) and climate variables, would be one important direction of decadal paleo-climate DA in the future. Meanwhile, quantifying uncertainties in proxy records and including multiple types of proxy records are also crucial to improve the reliability of the decadal paleo-climate DA.

Furthermore, potential discrepancies between proxy records and model simulations may also arise from the differences in the variables that are compared, e.g., oxygen and carbon isotopes from proxy records versus precipitation from model simulations. Therefore, the transient simulations using isotope-enabled earth system models facilitate direct comparisons and assimilations, with no transferring functions needed. However, this requires a deeper understanding of the physical mechanisms behind the changes in proxy records, and then identifying the analog in the model simulations [97].

4.3. Assessing the relative contribution of external vs internal variability

Currently, the DCPP is a coordinated multi-model investigation into decadal climate prediction, predictability, and variability, serving as a contribution to CMIP6 and WCRP Grand Challenge on Near Term Climate Prediction. As the key feature of DCPP, skillful decadal predictions require that both forced and internal components of the climate system are initialized, and diagnosing their individual contributions is also essential for improving the accuracy of decadal climate hindcasts and forecasts. Therefore, broader initial climatic conditions from the pre-industrial CE for such retrospective decadal predictions extracted could help overcome the limitations due to the scarcity of available observed data [96].

However, despite the studies on decadal climate variability and mechanisms during the CE, the relative contributions of external forcing and internal variability have not been fully addressed. Further study should continue on differentiating the relative role of external forcings and internal variability, and corresponding mechanisms. This requires deeper analyses of proxy reconstructions and model simulations, along with improvements in model structures on relevant ocean-atmosphere dynamics. For example, multivariate (MTM-SVD) analysis of the CESM-LME surface temperature fields both with and without forced component of variability removed, and additional and ideally larger true model simulation ensemble and expanded paleoclimate proxy data, could both provide more robust insights [84].

Differentiating the contributions from internal variability and external forcing could also help improve decadal prediction. For now, the lack of evidence for multidecadal oscillation distinct from red noise also raises questions for skillful decadal prediction, which relies on predictable internal variability [2]. As a result, the specification of external forcing contributes to the predictability of these forecasts [99,100]. However, a recent study found that including volcanic forcing in the prediction system significantly degrades the forecast skill of detrended multiyear-to-decadal SST variability in the central-eastern tropical Pacific [101].

In summary, future studies should combine the model improvements in representing the dynamics of decadal variability with longer-term paleo-climate proxy records with improved chronology and resolution [102]. In collaboration with other climate research communities, paleoclimate studies can advance our understanding of the decadal-scale internal variability of climate systems and responses to external forcings, and contribute to more accurate climate prediction and estimates of equilibrium climate sensitivity.

Conflict of interest

The authors declare that they have no conflict of interest.

Acknowledgments

This work was jointly supported by the National Key Research and Development Program of China (2023YFF0804700 and 2020YFA0608601), the Science and Technology Innovation Project of Laoshan Laboratory (LSKJ202203300), the Strategic Priority Research Program of the Chinese Academy of Sciences (XDB40000000), the National Natural Science Foundation of China (42130604, 42111530182, and 42075049), and Open Funds of State Key Laboratory of Loess and Quaternary Geology, Institute of Earth Environment, Chinese Academy of Sciences (SKLLQG1820 and SKLLQG1930).

Author contributions

Liang Ning, Zhengyu Liu, and Jian Liu conceived and designed the research. Liang Ning, Zhengyu Liu, and Michael E. Mann performed the experiments and analyses. Liang Ning, Kefan Chen, and Yanmin Qin prepared the figures. Liang Ning and Zhengyu Liu wrote the initial manuscript, and other authors contributed to the discussion of the results and co-wrote the paper.

Appendix A. Supplementary material

Supplementary data to this article can be found online at https://doi.org/10.1016/j.scib.2025.04.056.

References:

[1] Meehl GA, Richter JH, Teng H, et al. Initialized earth system prediction from subseasonal to decadal timescales. Nat Rev Earth Environ 2021;2:340–57.
[2] Mann ME, Steinman BA, Miller SK, et al. Absence of internal multidecadal and interdecadal oscillations in climate model simulations. Nat Commun 2020;11:49.
[3] Mann ME. Beyond the hockey stick: climate lessons from the Common Era. Proc Natl Acad Sci USA 2021;118:e2112797118.
[4] Liu Z. Dynamics of interdecadal climate variability: a historical perspective. J Clim 2012;25:1963–95.
[5] Liu Z, Di Lorenzo E. Mechanism and predictability of Pacific Decadal Oscillation. Curr Clim Change Rep 2018;4:128–44.
[6] Zhang R, Sutton R, Danabasoglu G, et al. A review of the role of the Atlantic meridional overturning circulation in Atlantic multidecadal variability and associated climate impacts. Rev Geophys 2019;57:316–75.
[7] Mann ME, Zhang Z, Rutherford S, et al. Global signatures and dynamical origins of the little ice age and medieval climate anomaly. Science 2009;326:1256–60.
[8] PAGES2k Consortium. Consistent multidecadal variability in global temperature reconstructions and simulations over the Common Era. Nat Geosci 2019; 12: 643–649.
[9] Tardif R, Hakim GJ, Perkins WA, et al. Last millennium reanalysis with an expanded proxy database and seasonal proxy modeling. Clim Past 2019;15:1251–73.
[10] Steiger NJ, Smerdon JE, Cook ER, et al. A reconstruction of global hydroclimate and dynamical variables over the Common Era. Sci Data 2018;5:180086.
[11] Neukom R, Steiger N, Gomez-Navarro J, et al. No evidence for globally coherent warm and cold periods over the preindustrial Common Era. Nature 2019;571:550–4.
[12] Newman M, Alexander MA, Ault TR, et al. The Pacific Decadal Oscillation, revisited. J Clim 2016;29:4399–427.
[13] Steinman BA, Mann ME, Miller SK, et al. Atlantic and Pacific multidecadal oscillations and Northern Hemisphere temperatures. Science 2015;347:988–91.
[14] Capotondi A, McGregor S, McPhaden MJ, et al. Mechanisms of tropical Pacific decadal variability. Nat Rev Earth Environ 2023;4:754–69.
[15] MacDonald GM, Case RA. Variations in the Pacific Decadal Oscillation over the past millennium. Geophys Res Lett 2005;32:L08703.
[16] D'Arrigo R, Wilson R. On the Asian expression of the PDO. Int J Climatol 2006;26:1607–17.
[17] D'Olivo JP, Zinke J, Goyal R, et al. Coral Sr/Ca-SST reconstruction from Fiji extending to ~1370 CE reveals insights into the Interdecadal Pacific Oscillation. Sci Adv 2024;10:eado5107.
[18] Vance TR, Roberts JL, Plummer CT, et al. Interdecadal Pacific variability and eastern Australian megadroughts over the last millennium. Geophys Res Lett 2015;42:129–37.
[19] Li S, Tian L, Cai Z, et al. A reconstructed PDO history from an ice core isotope record on the central Tibetan Plateau. npj Clim Atmos Sci 2024;7:270.
[20] Buckley BM, Ummenhofer CC, D'Arrigo RD, et al. Interdecadal Pacific Oscillation reconstructed from trans-Pacific tree rings: 1350-2004 CE. Clim Dyn 2019;53:3181–96.
[21] Porter SE, Thompson EM, Thompson LG, et al. Reconstructing an interdecadal Pacific oscillation index from a Pacific basin-wide collection of ice core records. J Clim 2021;34:3839–52.
[22] Wise EK. Tropical Pacific and Northern Hemisphere influences on the coherence of Pacific Decadal Oscillation reconstructions. Int J Climatol 2015;35:154–60.
[23] Henley BJ. Pacific decadal climate variability: indices, patterns and tropical-extratropical interactions. Glob Planet Change 2017;155:42–55.
[24] Fang C, Wu L, Zhang X. The impact of global warming on the Pacific decadal oscillation and the possible mechanism. Adv Atmos Sci 2014;31:118–30.
[25] Li J, Sun C, Jin FF. NAO implicated as a predictor of Northern Hemisphere mean temperature multidecadal variability. Geophys Res Lett 2013;40:5497–502.
[26] Sun C, Li J, Jin FF. A delayed oscillator model for the quasi-periodic multidecadal variability of the NAO. Clim Dyn 2015;45:2083–99.
[27] Gray ST, Graumlich JL, Betancourt JL, et al. A tree-ring based reconstruction of the Atlantic Multidecadal Oscillation since 1567 A.D. Geophys Res Lett 2004;31:L12205.
[28] Wang J, Yang B, Ljungqvist FC, et al. Internal and external forcing of the multidecadal Atlantic climate variability over the past 1200 years. Nat Geosci 2017;10:512–8.
[29] Lapointe F, Bradley RS, Francus P, et al. Annually resolved Atlantic sea surface temperature variability over the past 2900 y. Proc Natl Acad Sci 2019;117:27171–8.

[30] Mann ME, Steinman BA, Brouillette DJ, et al. Multidecadal climate oscillations during the past millennium driven by volcanic forcing. Science 2021;371:1014–9.
[31] Sun C, Zhang J, Li X, et al. Atlantic meridional overturning circulation reconstructions and instrumentally observed multidecadal climate variability: a comparison of indicators. Int J Climatol 2021;41:763–78.
[32] Zhang J, Liu Y, Sun C, et al. On the connection between AMOC and observed land precipitation in Northern Hemisphere: a comparison of the AMOC indicators. Clim Dyn 2021;56:651–64.
[33] Gong Z, Liu Y, Sun C, et al. Linking AMOC variations with the multidecadal seesaw in tropical cyclone activity between eastern North Pacific and Atlantic. J Geophys Res Oceans 2021;126:e2021JC017308.
[34] Caesar L, Mccarthy GD, Thornalley D, et al. Current Atlantic meridional overturning circulation weakest in last millennium. Nat Geosci 2021;14:118–20.
[35] Zhu C, Liu Z. Weakening Atlantic overturning circulation causes South Atlantic salinity pile-up. Nat Clim Change 2020;10:998–1003.
[36] Fu Y, Li F, Karstensen J, et al. A stable Atlantic Meridional Overturning Circulation in a changing North Atlantic Ocean since the 1990s. Sci Adv 2020;6:eabc7836.
[37] Moffa-Sanchez P, Hall IR. North Atlantic variability and its links to European climate over the last 3000 years. Nat Commun 2017;8:1726.
[38] Thibodeau B, Not C, Zhu J, et al. Last century warming over the Canadian Atlantic shelves linked to weak Atlantic meridional overturning circulation. Geophys Res Lett 2018;45:376–85.
[39] Thornalley DJ, Oppo DW, Ortega P, et al. Anomalously weak Labrador Sea convection and Atlantic overturning during the past 150 years. Nature 2018;556:227–30.
[40] Trouet V, Scourse JD, Raible CC, et al. North Atlantic storminess and Atlantic meridional overturning circulation during the last millennium: reconciling contradictory proxy records of NAO variability. Glob Planet Change 2012;84:48–55.
[41] Lapointe F, Bradley RS. Little ice age abruptly triggered by intrusion of Atlantic waters into the Nordic seas. Sci Adv 2021;7:eabi8230.
[42] Mimi MS, Liu W. Atlantic meridional overturning circulation slowdown modulates wind-driven circulations in a warmer climate. Commun Earth Environ 2024;5:727.
[43] Li J, Xie SP, Cook ER, et al. El Nino modulations over the past seven centuries. Nat Clim Change 2013;3:822–6.
[44] Ruprich-Robert Y, Msadek R, Castruccio F, et al. Assessing the climate impacts of the observed Atlantic multidecadal variability using the GFDL CM2.1 and NCAR CESM1 global coupled models. J Clim 2017;30:2785–810.
[45] Levine AFZ, McPhaden MJ, Frierson DMW. The impact of the AMO on multidecadal ENSO variability. Geophys Res Lett 2017;44:3877–86.
[46] Gan R, Liu Q, Huang G, et al. Greenhouse warming and internal variability increase extreme and central Pacific El Niño frequency since 1980. Nat Commun 2023;14:394.
[47] Geng X, Zhang W, Jin F, et al. Modulation of the relationship between ENSO and its combination mode by the Atlantic multidecadal oscillation. J Clim 2020;33:4679–95.
[48] Zhang Y, Wang W, Ding R, et al. Modulation of the predictability of the East Asian summer monsoon by the interdecadal Pacific oscillation. J Geophys Res Atmos 2022;127:e2021JD035903.
[49] Ding R, Nnamchi HC, Yu JY, et al. North Atlantic oscillation controls multidecadal changes in the North Tropical Atlantic-Pacific connection. Nat Commun 2023;14:862.
[50] Du X, Dee S, Hu J, et al. Solar irradiance modulates the Asian summer monsoon - ENSO relationship over the last millennium. Geophys Res Lett 2023;50:e2023GL105708.
[51] Zheng J, Wang W, Ge Q, et al. Precipitation variability and extreme events in eastern China during the past 1500 years. Terr Atmos Ocean Sci 2006;17:579–92.
[52] Shi F, Guo Z, Goosse H, et al. Multi-proxy reconstructions of May–September precipitation field in China over the past 500 years. Clim Past 2017;13:1919–38.
[53] Shi H, Wang B, Liu J, et al. Decadal-multidecadal variations of Asian summer rainfall from the little ice age to the present. J Clim 2019;32:7663–74.
[54] Cook ER, Anchukaitis KJ, Buckley BM, et al. Asian monsoon failure and megadrought during the last millennium. Science 2010;328:486–9.
[55] Sinha A, Berkelhammer M, Stott L, et al. The leading mode of Indian summer monsoon precipitation variability during the last millennium. Geophys Res Lett 2011;38:L15703.
[56] Shi F, Fang K, Xu C, et al. Interannual to centennial variability of the South Asian summer monsoon over the past millennium. Clim Dyn 2017;49:2803–14.
[57] Sinha A, Kathayat G, Cheng H, et al. Trends and oscillations in the Indian summer monsoon rainfall over the last two millennia. Nat Commun 2015;6:6309.
[58] Feng S, Hu Q. How the North Atlantic multidecadal oscillation may have influenced the Indian summer monsoon during the past two millennia. Geophys Res Lett 2008;35:L01707.
[59] Fan F, Mann ME, Ammann CM, et al. Understanding changes in the Asian summer monsoon over the past millennium: insights from a long-term coupled model simulation. J Clim 2009;22:1736–48.
[60] Kumar KK, Rajagopalan B, Cane MA, et al. On the weakening relationship between the Indian Monsoon and ENSO. Science 1999;284:2156–9.
[61] Zhou T, Gong D, Li J, et al. Detecting and understanding the multi-decadal variability of the East Asian Summer Monsoon - Recent progress and state of affairs. Meteorol Z 2009;18:455–67.
[62] Wang Q, Yan M, Liu J, et al. Impacts of land use/cover change on spatial patterns of summer precipitation at decadal scale over Eastern China. Int J Climatol 2021;41:1939–51.
[63] Shi F, Goosse H, Li J, et al. Interdecadal to multidecadal variability of East Asian summer monsoon over the past half millennium. J Geophys Res Atmos 2022;127:e2022JD037260.
[64] Ge Q, Fang X, Zheng J. Learning from the historical impacts of climatic change in China. Adv Earth Sci 2014;29:23–9.
[65] Ning L, Chen K, Liu J, et al. How do the volcanic eruptions influence the decadal megadrought over the eastern China? J Clim 2020;33:8195–207.
[66] Wang K, Zhao J, Wang J, et al. Past decadal climate variability of East Asian summer monsoon: characteristics and mechanisms. Chin Sci Bull 2025;70:240–61 (in Chinese).
[67] Wang T, Ottera OH, Gao Y, et al. The response of the North Pacific decadal variability to strong tropical volcanic eruptions. Clim Dyn 2012;39:2917–36.
[68] Liu W, Shi F, Xiao G, et al. Bidecadal temperature anomalies over the Tibetan Plateau and Arctic in response to the 1450s volcanic eruptions. J Geophys Res Atmos 2022;127:e2021JD035769.
[69] Man W, Zhou T, Jungclaus JH. Effects of large volcanic eruptions on global summer climate and East Asian Monsoon changes during the last millennium: analysis of MPI-ESM simulations. J Clim 2014;27:7394–409.
[70] Chen K, Ning L, Liu Z, et al. One drought and one volcanic eruption influenced the history of China: the Ming Dynasty Megadrought. Geophys Res Lett 2022;47:e2020GL088124.
[71] Chen K, Ning L, Liu Z, et al. Nonlinear responses of droughts over China to volcanic eruptions at different drought phases. Geophys Res Lett 2022;49: e2021GL096454.
[72] Dai Z, Wang B, Zhu L, et al. Atlantic multidecadal variability response to external focing during the past two millennia. J Clim 2022;35:4503–15.
[73] Ning L, Liu J, Sun W, et al. Influences of volcano eruptions on Asian Summer Monsoon over the last 110 years. Sci Rep 2017;7:42626.
[74] Xue J, Ning L, Qin Y, et al. Comparisons on characteristics and mechanisms of the decadal megadroughts over eastern China between MCA and LIA. Int J Climatol 2021;41:1985–97.
[75] Xue J, Ning L, Liu Z, et al. The combined influences of solar radiation and PDO on precipitation over eastern China during the last Millennium. Clim Dyn 2023;60:1137–50.
[76] Wang L, Ning L, Chen K, et al. Influence and mechanism of solar radiation intensity on the interdecadal variability of strong Meiyu events during historical periods. Sci China Earth Sci 2023;66:408–16.
[77] Qin Y, Ning L, Li L, et al. Assessing the modern multi-decadal scale aridification over the Northern China from a historical perspective. J Geophys Res Atmos 2022;127:e2021JD035622.
[78] Cheng J, Liu Z, Zhang S, et al. Reduced interdecadal variability of Atlantic meridional overturing circulation under global warming. Proc Natl Acad Sci USA 2016;113:3175–8.
[79] Ma X, Liu W, Burls NJ, et al. Evolving AMOC multidecadal variability under different CO_2 forcings. Clim Dyn 2021;57:593–610.
[80] Qin Y, Ning L, Li L, et al. Future risk of decadal megadrought events over eastern China based on IPO-constrained precipitation. Clim Dyn 2024;62:2227–38.
[81] He C, Clement AC, Kramer SM, et al. Tropical Atlantic multidecadal variability is dominated by external forcing. Nature 2023;622:521–7.
[82] Liu Z, Gu P, Delworth T, et al. Strong red noise ocean forcing on Atlantic Multidecadal Variability assessed from surface heat flux: theory and application. J Clim 2023;36:53–80.
[83] Crowley TJ. Causes of climate change over the past 1000 years. Science 2000;289:270–7.
[84] Mann ME, Steinman BA, Brouillette DJ, et al. On the estimation of internal climate variability during the preindustrial past millennium. Geophys Res Lett 2022;49:e2021GL096596.
[85] Waple A, Mann ME, Bradley RS, et al. Long-term patterns of solar irradiance forcing in model experiments and proxy-based surface temperature reconstructions. Clim Dyn 2022;18:563–78.
[86] Yan X, Zhang R, Knutson TR, et al. A multivariate AMV index and associated discrepancies between observed and CMIP5 externally forced AMV. Geophys Res Lett. 2020;46:4421–31.
[87] Pausata FS, Chafik L, Caballero R, et al. Impacts of high-latitude volcanic eruptions on ENSO and AMOC. Proc Natl Acad Sci USA 2015;112:13784–8.
[88] Chen K, Ning L, Liu Z, et al. Modulating and resetting impacts of different volcanic eruptions on North Atlantic SST variations. J Geophys Res Atmos 2022;127:e2021JD036246.
[89] Elsbury D, Peings Y, Saint-Martin D, et al. The atmospheric response to positive IPV, positive AMV, and their combination in boreal winter. J Clim 2019;32:4193–213.
[90] Zhang R, Delworth TL. Impact of the Atlantic multidecadal oscillation on North Pacific climate variability. Geophys Res Lett 2007;34:L23708.
[91] Sun C, Kucharski F, Li J, et al. Western tropical Pacific multidecadal variability forced by the Atlantic multidecadal oscillation. Nat Commun 2017;8:15998.
[92] An X, Wu B, Zhou T, et al. Atlantic multidecadal oscillation drives interdecadal Pacific variability via tropical atmosphere bridge. J Clim 2021;34:5543–53.
[93] Li X, Xie S, Gille ST, et al. Atlantic-induced pan-tropical climate change over the past three decades. Nat Clim Change 2015;6:275–80.

[94] Meehl GA, Hu A, Castruccio F, et al. Atlantic and Pacific tropics connected by mutually interactive decadal-timescale processes. Nat Geosci 2021;14:36–42.
[95] Hong J, Yeh S, Yang Y, et al. Interbasin interactions between the Pacific and Atlantic Oceans depending on the phase of Pacific decadal oscillation and Atlantic multidecadal oscillation. J Clim 2022;35:2883–94.
[96] Goose H, Klein F, Swingedouw D, et al. Internal and forced decadal variability: lessons from the past millennium. PAGEs Mag 2017;25:47–51.
[97] Liu Z, Bao Y, Thompson LG, et al. Tropical mountain ice core $\delta^{18}O$: a goldilocks indicator for global temperature change. Sci Adv 2023;9:eadi6725.
[98] Ault TR. Reconciling disparate views on decadal climate variability from proxies and models. PAGEs Mag 2017;25:68–70.
[99] Zhou TJ, Zuo M, Man WM. Recent advances and future avenues in examining the impacts of volcanic aerosols on climate. Chin Sci Bull 2024;69:230–52 (in Chinese).
[100] Mann ME et al. Predictability of the recent slowdown and subsequent recovery of large-scale surface warming using statistical methods. Geophys Res Lett 2016;43:3459–67.
[101] Wu X, Yeager SG, Deser C, et al. Volcanic forcing degrades multiyear-to-decadal prediction skill in the tropical Pacific. Sci Adv 2023;9:eadd9364.
[102] Liu Y. Example of near-term decadal climate trend prediction based on tree-ring data. Chin Sci Bull 2021;66:3474–9 (in Chinese).